

Effects of Zn content on the magnetic and magnetocaloric properties of Ni-Zn ferrites

N. Chau¹, N.K. Thuan¹, D.L. Minh², N.H. Luong^{1,*}

¹ Center for Materials Science, College of Science, VNU, 334 Nguyen Trai, Hanoi, Vietnam

² Department of Solid State Physics, College of Science, VNU, 334 Nguyen Trai, Hanoi, Vietnam

Received 20 August 2008

Abstract. Among spinel ferrites, Cd and Zn ferrites are always normal ferrites with Cd and Zn ions locating only in tetrahedral sites. This study presents effect of Zn on the magnetic and magnetocaloric properties of the mixed spinel ferrites $\text{Ni}_{1-x}\text{Zn}_x\text{Fe}_2\text{O}_4$ ($x = 0.60, 0.65, 0.70, 0.75$). The presence of Zn affects lattice parameters, saturation magnetization M_s , Curie temperature, T_c , and magnetic entropy change ΔS_m . At highest Zn content, T_c reduces to the temperature lower than room temperature and magnetic structure of spins in the octahedral sublattice should be strongly canted. The maximum magnetic entropy change occurs in a large temperature range from low temperature to hundreds of Celsius degrees.

Keywords: ferrite, magnetocaloric effect.

1. Introduction

It is well known that spinel ferrites consist of three types of magnetic structures: normal, inverse and mixed spinel [1]. In normal spinel, the divalent ions locate at tetrahedral sublattice (A-site) and trivalent ions Fe^{3+} locate at octahedral sublattice (B-site). In inverse spinel a half of Fe^{3+} ions locates at A site and the rest Fe^{3+} ions together with divalent ions locate at B site. In mixed spinel ferrite, both Fe^{3+} ions and divalent ions locate at A and B site. NiFe_2O_4 is inverse spinel ferrite. Among spinel ferrites, only Zn and Cd ferrites belong to pure normal structure. Mixed Ni-Zn ferrites have extremely high resistivity so that they are widely used as soft magnetic materials suitable for high-frequency applications. Initial permeability is maximum at 30 mol % NiFe_2O_4 , 70 mol % ZnFe_2O_4 and this composition has Curie temperature, T_c , near room temperature [2]. For the theoretical examination of properties of ferrites it could be started from the parameters characterizing for superexchange interaction types A-A, B-B, A-B. Interaction A-A belongs to neighbor magnetic ions in sublattice A, interaction B-B - between ions in sublattice B and interaction A-B - between ions of sublattices A and B. We denote λ_{aa} , λ_{bb} , λ_{ab} correspond to molecular-field constants of exchange interaction A-A, B-B and A-B, respectively [3].

Exchange interactions between magnetic ions through oxygen ion are superexchange interaction with antiferromagnetic nature. These interactions depend on bond distance and bond length. Normally

* Corresponding author. Fax: (84-4) 3858 9496
Email: luongnh@vnu.edu.vn

$|\lambda_{ab}| \gg |\lambda_{bb}| > |\lambda_{aa}|$, therefore magnetic moments of A sublattice is antiparallel oriented with spins in B sublattice [4]. The increase of Zn content in Ni-Zn ferrites makes weakening λ_{ab} and could lead to canting structure in B site [3]. Usually canting structure of ferrites was examined by neutron scattering.

The studies on spinel ferrites were started long time ago but recently a large number of publications dealing with them has been performed including nanoparticles and thin ferrite films [5-12]. Especially, superparamagnetic properties of Ni-Zn ferrite for nano-bio fusion applications were reported [13].

In this paper we study magnetic and electric properties including canting structure of Ni-Zn ferrites with high Zn content and at the first time we attempted to observe magnetocaloric effect (MCE) in these ferrites.

2. Experiments

The polycrystalline ferrite samples $\text{Ni}_{1-x}\text{Zn}_x\text{Fe}_2\text{O}_4$ ($x = 0.60; 0.65; 0.70$ and 0.75) were prepared by standard solid state reaction technique. The mixed powders were presintered at 900°C for 3 hours and then reground to the fine particles, pressed into pellets and again heated at 900°C for 3 hours. The second reground powders were pressed and sintered at 1300°C for 3 hours. The crystal structure of samples was checked by X-ray diffractometer D5005, Bruker and the microstructure of samples was examined by Scanning Electron Microscope (SEM) Jeol LV5410. Magnetic properties of ferrites were measured by Vibrating Sample Magnetometer DMS 880, Digital Measurement System. Resistivity measurements were performed by four probe method.

3. Results and discussion

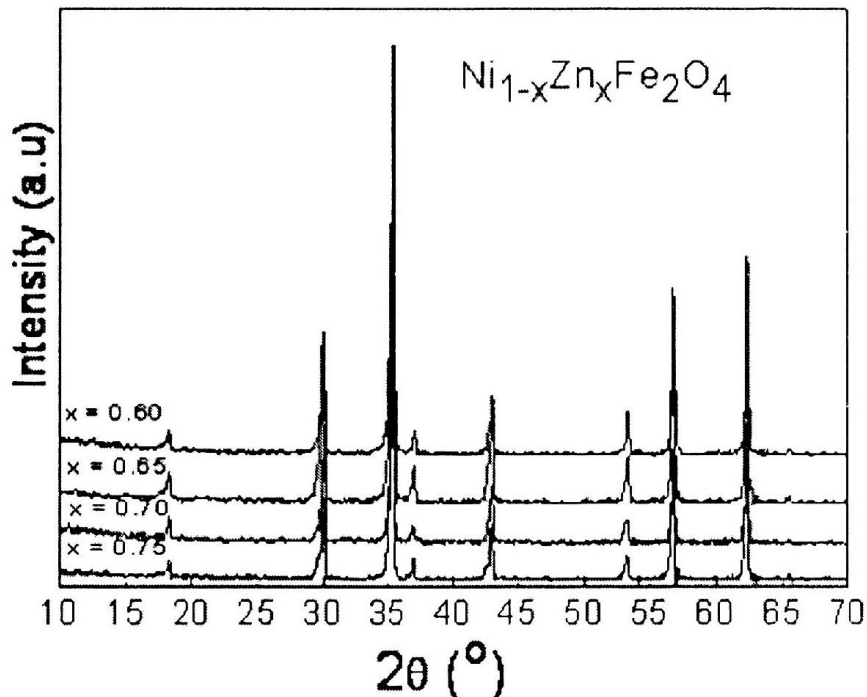


Fig. 1. X-ray diffraction patterns of ferrite samples $\text{Ni}_{1-x}\text{Zn}_x\text{Fe}_2\text{O}_4$.

The SEM study showed that the microstructure of samples is of high homogeneity and average particle size increases with Zn content in samples, namely from 2.1 μm (x = 0.60) to 2.8 μm (x = 0.65) to 2.9 μm (x = 0.70) and to 3.1 μm (x = 0.75). Fig. 1 presents the XRD patterns of studied samples. All samples have single phase f.c.c spinel structure and lattice parameters are determined and listed in Tab. 1. It is clear from this table that lattice constant and volume of unit cell increase with Zn content in the samples due to larger ionic radius of Zn²⁺ ion (0.82 Å) substituted for Ni²⁺ ion (0.78 Å).

The X-ray density, the real density as well as porosity of ferrites also determined and illustrated in Tab. 1. While the X-ray density is slightly decreased with increasing Zn content in samples (due to the extension of unit cell), the real density of samples enhanced because of reducing of porosity from 15.1 % (x = 0.60) to 7.6 % (x = 0.75).

Table 1. Lattice parameters, X-ray density, real density and porosity of samples Ni_{1-x}Zn_xFe₂O₄

Sample	Ni _{1-x} Zn _x Fe ₂ O ₄			
	x = 0.60	X = 0.65	x = 0.70	x = 0.75
a (Å)	8.4108	8.4149	8.4208	8.4251
V (Å ³)	594.99	595.86	597.12	598.03
D _x (g/cm ³)	5.322	5.321	5.318	5.317
D (g/cm ³)	4.52	4.65	4.82	4.92
P (%)	15.1	12.6	9.4	7.6

In highest Zn content sample (x = 0.75) the crystal boundary became narrower due to development of particle size. Because ZnO has low melting temperature so in high ZnO content sample, the liquid phase easy to perform at high sintering temperature and eliminates the porosity of ferrite.

The magnetization curves of all samples have been measured at 110 K in maximal applied field of 13.5 kOe. The results showed that at this field the studied samples are nearly in saturation and saturation magnetization of samples is listed in Tab. 2. From the shape of measured M(T) curves, we should approximately suppose that these values correspond to saturation magnetization of samples at 0 K.

As we known, NiZn ferrites are inverse spinel with following orientation of spins [1-3]:



and according to Neel theory [4] saturation magnetization for formula unit could be determined by expression:

$$M_{Sr} = [2(1-x)\mu_B + 5(1+x)\mu_B] - 5(1-x)\mu_B = (2+8x)\mu_B \tag{2}$$

where Zn²⁺ ion is nonmagnetic ion, Ni²⁺ has 2μ_B, Fe³⁺ has 5 μ_B and x is Zn amount containing in ferrite. Saturation magnetization M_{Sr} calculated from formula (2) and M_{Se} measured for formula unit are showed in Tab. 2.

The saturation magnetization M_{Sr} calculated with assuming that exchange interaction λ_{ab} is strongest therefore magnetic moments of A and B sublattices are antiparallel to each other and M_{Sr} increases with x. In fact M_{Se} measured in experiment decreased with x. It means that with increasing Zn content in ferrite, A-B interaction became weakening so should be compared with B-B interaction and we suppose in our studied samples there is canting structure as illustrated in Fig. 2, where φ is the angle between direction of magnetic moment of A ions and magnetic moment of B₁ and B₂ ions. Comparing M_{Sr} and M_{Se} from Tab. 2, we could determine the canting angle between magnetic moments of B₁ and B₂ ions in octahedral sublattice. We see that canting angle increases with increasing amount of nonmagnetic ions Zn²⁺ in ferrite which causes weakening exchange interactions.

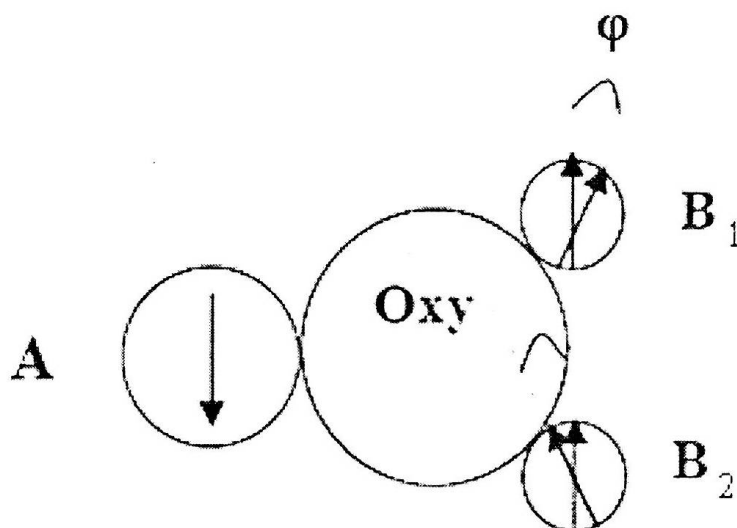


Fig. 2. Canting structure of NiZn ferrite when λ_{ab} , λ_{bb} and λ_{aa} have the same order.

Table 2. Saturation magnetization and canting angle of ferrites $Ni_{1-x}Zn_xFe_2O_4$

x	0.60	0.65	0.70	0.75
I_s (emu/g)	112.8	99.68	95.36	74.43
M_{st} (μ_B)	6.8	7.2	7.6	8.0
M_{se} (μ_B)	4.59	4.26	4.08	3.19
φ_c ($^\circ$)	41.5	47.8	52.1	61.3

In order to study the spin order and magnetic behavior of samples, the field-cooled (FC) and zero field-cooled (ZFC) magnetization measurements were performed in magnetic field of 20 Oe (Fig. 3). The FC and ZFC curves depart from each other below the freezing temperature T_f indicating the onset of blocking of clusters. The sample settles into the frozen state below temperature T_f . This behavior is attributed to the magnetic frustration arising from the co-existence of competing antiferromagnetic and ferromagnetic interactions. The separation of FC and ZFC curves at low temperatures could be considered that the sample exhibits cluster glass-like state. This behavior has been observed for all studied ferrites. From the data of Fig. 3, the Curie temperature T_c has been determined based on Arrott plots and listed in Tab. 3.

Table 3. Curie temperature, T_m and maximum value of magnetic entropy change of ferrites $Ni_{1-x}Zn_xFe_2O_4$

X	0.60	0.65	0.70	0.75
T_c	407	360	305	260
T_m^* (K)	387	345	300	265
$ \Delta S_m _{max}$ (J/kg.K)	0.88	0.84	0.98	0.88

*) T_m is temperature at which $|\Delta S_m|$ reaches a maximum.

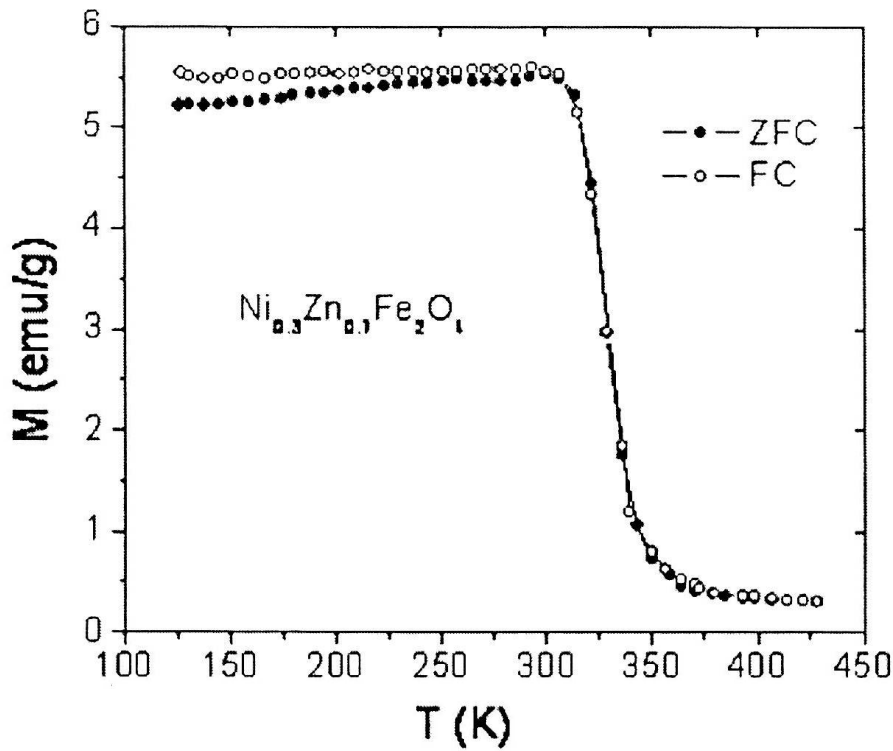


Fig. 3. FC and ZFC thermomagnetic curves of ferrite $Ni_{0.3}Zn_{0.7}Fe_2O_4$.

It is clearly seen from this table that T_C decreases with increasing Zn content substituted for Ni in ferrites and is around room temperature for ferrite $Ni_{0.3}Zn_{0.7}Fe_2O_4$. The reduction of T_C here could be explained by weakening exchange interaction mainly between magnetic ions in sublattices A and B.

As we well known, the adiabatic magnetic entropy change, ΔS_m , is determined by Maxwell's fundamental relation [14]:

$$\Delta S_m(T, \Delta H) = \int_0^{H_{max}} \left(\frac{\partial M(T, H)}{\partial T} \right)_H dH \quad (3)$$

where H_{max} is the final applied magnetic field. To study the MCE of samples, a series of isothermal magnetization curves around their respective T_C has been measured in a magnetic field up to 13.5 kOe. Fig. 4 a shows these curves of ferrite $Ni_{0.3}Zn_{0.7}Fe_2O_4$.

When magnetization is measured in a small discrete field and temperature interval, ΔS_m could be determined from Eq. (3) by expression:

$$\Delta S_m = \sum \frac{M_i - M_{i+1}}{T_i - T_{i+1}} \Delta H \quad (4)$$

where M_i and M_{i+1} are the experimental values of magnetization at T_i and T_{i+1} , respectively, under magnetic field variation of ΔH .

The $|\Delta S_m|(T)$ curve of ferrite $Ni_{0.3}Zn_{0.7}Fe_2O_4$ is illustrated in Fig. 4 b and $|\Delta S_m|$ reached a maximum value of 0.98 J/kg.K near Curie temperature. Similar behavior was observed for other samples investigated and the results are listed in Table 3. The values of $|\Delta S_m|_{max}$ in our samples are identify with that firstly examined by Chaudhary et al. [15] for cobaltite perovskites $La_{1-x}Sr_xCoO_3$. Thus $Ni_{1-x}Zn_xFe_2O_4$ ($x = 0.60; 0.65; 0.70; 0.75$) ferrites could be considered as active magnetic refrigerant materials working in quite wide temperature range.

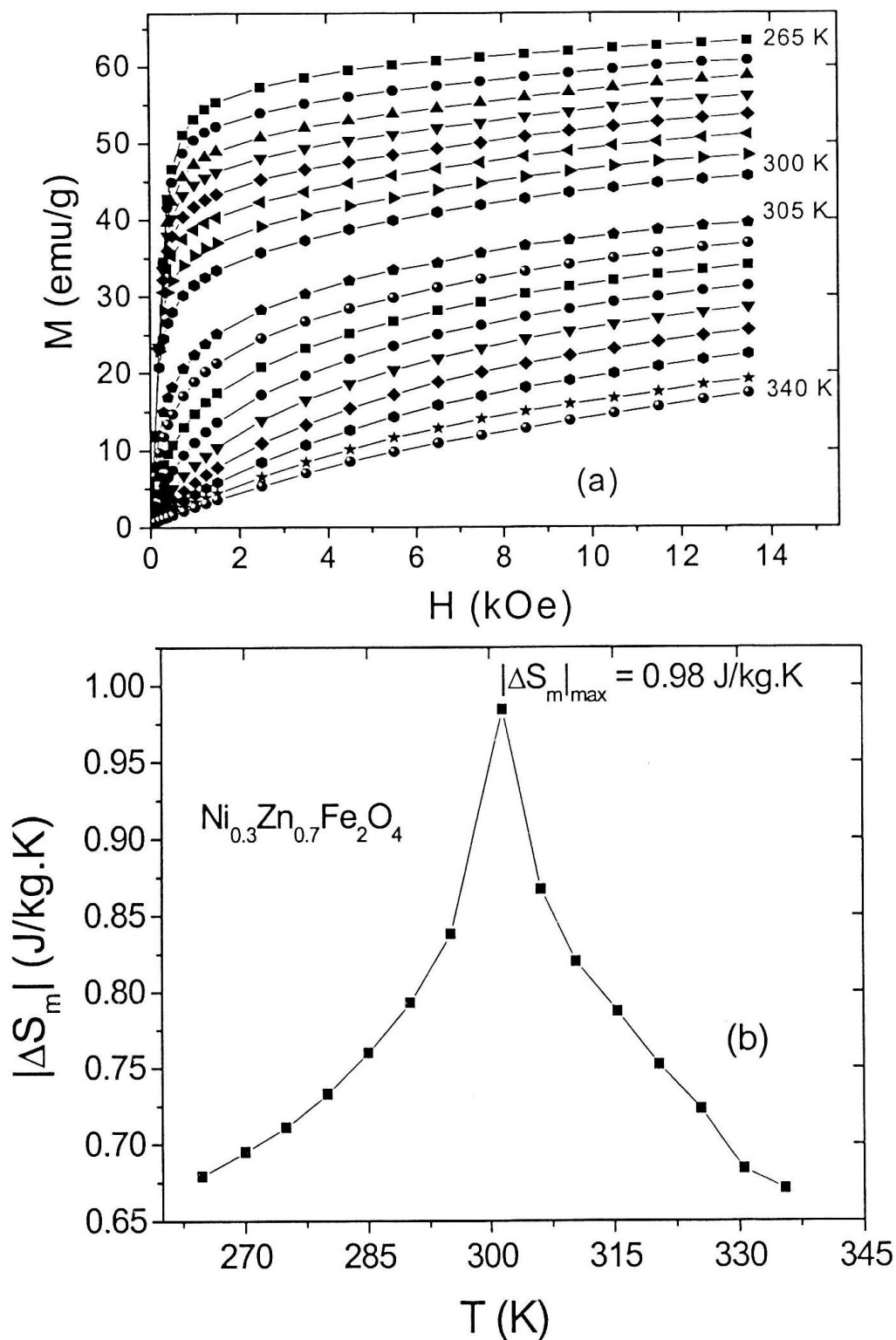


Fig. 4. (a) A series of isothermal magnetization curves and (b) magnetic entropy change $|\Delta S_m|$ versus temperature of sample $\text{Ni}_{0.3}\text{Zn}_{0.7}\text{Fe}_2\text{O}_4$.

Note that large MCE in manganite perovskites [16-19] and colossal MCE in amorphous alloys [20-23] have been examined by us.

The resistance of samples has been measured in the temperature region from 125 K to 300 K and the linear dependence of $\ln\rho$ on $1/T$ for ferrite $\text{Ni}_{0.3}\text{Zn}_{0.7}\text{Fe}_2\text{O}_4$ has been obtained and Fig. 5 shows this result as an example.

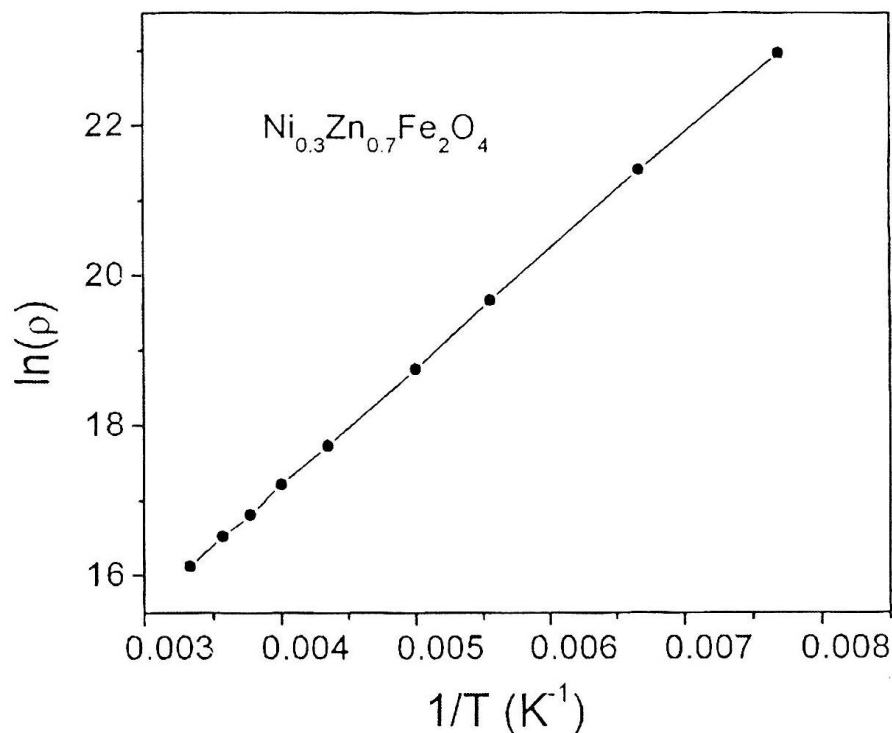


Fig. 5. Dependence of $\ln\rho$ on $1/T$ for ferrite $\text{Ni}_{0.3}\text{Zn}_{0.7}\text{Fe}_2\text{O}_4$.

Obviously, temperature dependence of resistivity of ferrites follows the below expression [1,2]:

$$\rho = \rho_0 e^{E_p/kT} \quad (5)$$

From Fig. 3 we could calculate activation energy E_p of $\text{Ni}_{0.3}\text{Zn}_{0.7}\text{Fe}_2\text{O}_4$ ferrite and the result showed to be 0.15 eV which corresponds to electron conductivity of ferrite [1]. The similar results are obtained for the rest studied ferrites.

4. Conclusions

Single phase ferrites $\text{Ni}_{1-x}\text{Zn}_x\text{Fe}_2\text{O}_4$ ($x = 0.60; 0.65; 0.70$ and 0.75) have been prepared with cluster glass-like state. The canting angles of magnetic moments in octahedral sublattice were approximately determined and that angle increases with Zn content in NiZn ferrite. At the first time we have examined the magnetocaloric effect in ferrite generally and the obtained $|\Delta S_m|_{\max}$ could be compared with that of perovskite. Moreover the temperature at which $|\Delta S_m|$ reached a maximum could be easily controlled by substitution effect.

Acknowledgements. The authors are grateful to the Vietnam National Fundamental Research Program (Project 406006) for the financial support.

References

- [1] J. Smit and H.P.J. Wijn, Ferrites (Wiley, New York, 1959).
- [2] T. Tsushima, T. Teranishi and K. Ohta, Handbook on the magnetic substances (ed. by S. Chikazumi et al., Akasura Publishing Co, Tokyo, 1975).

- [3] B. Lax, K.J. Button, Microwave ferrites and ferrimagnetics, McGraw-Hill Book Comp., Inc., New York, San Francisco, Toronto, London 1962.
- [4] L. Neel, *Ann. de Phys.* 3 (1948) 137.
- [5] A.S. Albuquerque, J.D. Ardisson, W.A.A. Macedo, *J. Appl. Phys.* 87 (2000) 4352.
- [6] A. Verma, T.C. Goel, R.G. Mendisata, *Mater. Sci. Tech.* 16 (2000) 712.
- [7] S.E. Jacobo, S. Duhalde, H.R. Bertorello, *J. Magn. Magn. Mater.* 272-276 (2004) 2253.
- [8] S.W. Lee, C.S. Kim, *J. Magn. Magn. Mater.* 303 (2006) e315.
- [9] J.H. Yin, J. Ding, J.S. Chen, X.S. Miao, *J. Magn. Magn. Mater.* 303 (2006) e387.
- [10] H.H. Nien, T.J. Liang, C.K. Huang, S.K. Changchien, *J. Magn. Magn. Mater.* 304 (2006) e204.
- [11] H.H. Nien, T.J. Liang, C.K. Huang, S.K. Changchien, *J. Magn. Magn. Mater.* 304 (2006) 2409.
- [12] H.T. Chan, Y.Y. Do, P.L. Huang, P.L. Chien, T.S. Chan, R.S. Liu, C.Y. Huang, S.Y. Yang, H.E. Horng, *J. Magn. Magn. Mater.* 304 (2006) e415.
- [13] S.W. Lee, C.S. Kim, *J. Magn. Magn. Mater.* 304 (2006) e418.
- [14] A.H. Morish, *The Physical Principles of Magnetism*, Willey, New York, 1963 (Chapter 3).
- [15] S. Chaudhary, V.S. Kumar, S.B. Roy, P. Chaddah, S.R. Krishnakumar, V.G. Sathe, A. Kumar, D.D. Sarma, *J. Magn. Magn. Mater.* 202 (1999) 47.
- [16] N. Chau, D.T. Hanh, N.D. Tho, N.H. Luong, *J. Magn. Magn. Mater.* 303 (2006) e335.
- [17] N. Chau, N.D. Tho, N.H. Luong, B.H. Giang, B.T. Cong, *J. Magn. Magn. Mater.* 303 (2006) e402.
- [18] D.T. Hanh, N. Chau, N.H. Luong, N.D. Tho, *J. Magn. Magn. Mater.* 304 (2006) e325.
- [19] D.T. Hanh, M.S. Islam, F.A. Khan, D.L. Minh, N. Chau, *J. Magn. Magn. Mater.* 310 (2007) 2826.
- [20] N. Chau, P.Q. Thanh, N.Q. Hoa, N.D. Tho, *J. Magn. Magn. Mater.* 304 (2006) 36.
- [21] N. Chau, N.Q. Hoa, N.D. Tho, P.Q. Niem, *J. Magn. Magn. Mater.* 304 (2006) e179.
- [22] N. Chau, N.D. Tho, N.Q. Hoa, C.X. Huu, N.D. Tho, S-C. Yu, *Mater. Sci. Eng.* A499-451 (2007) 360.
- [23] N.Q. Hoa, N. Chau, S-C. Yu, T.M. Thang, N.D. Tho, N.D. Tho, *Mater. Sci. Eng.* A449-451 (2007) 364.